Supporting Information

Design of pH-responsive polymer monolith based on cyclodextrin vesicle for capture and release of myoglobin

Haijiao Zheng [a], Xiqian Li [b], Qiong Jia [a, *]

[a] College of Chemistry, Jilin University, Changchun 130012, China

[b] China-Japan Hospital of Jilin University, Changchun 130033, China

Supporting Information Index:

* Corresponding author.
E-mail address: jiaqiong@jlu.edu.cn (Q. Jia)

1. Reagents and instrumentation

GMA, PETA, γ-methacryloxypropyl trimethoxysilane (γ-MAPS), Myo (≥ 95%, essentially salt-free, lyophilized powder), Traut's reagent, bovine serum albumin (BSA), trypsin, 1-adamantanecarboxylic acid, and dimethylol propionic acid (DMPA) were purchased from Sigma-Aldrich Company (St, Louis, MO, USA). Polyethylene glycol (PEG 6000 and PEG 20000), ethylene diamine tetraacetic acid (EDTA), and β-CD were acquired from Aladdin Reagent Company (Shanghai, China). Peptide-N-glycosidase (PNGase F), Traut's reagent, and octapeptide were from Biomiga Company (Shanghai, China). Sodium hydroxide (NaOH), hydrochloric acid (HCl), methanol (MeOH), acetonitrile (ACN), ethanol, acetone, trichloromethane ($CHCl_3$), phosphate buffered saline (PBS, pH 7.4), trifluoroacetic acid (TFA), formic acid (FA), and ammonium bicarbonate (NH_4HCO_3) were obtained from Tianjin Guangfu Fine Chemical Research Institute (Tianjin, China). Water was purified by a Milli-Q system (Millipore, MA, USA). GMA and PETA were distilled under vacuum before use. AIBN was purified by recrystallizatiocn from ethanol and dried under vacuum at room temperature prior to use. All the other reagents were used as received.

Fused-silica capillaries (530 μm i. d.) were purchased from Yongnian Optical Fiber Factory (Handan, China). A precise syringe pump (GT0785, USA) was used to push liquids through monoliths. A KQ-200KDE digital ultrasonic cleaner was obtained from Kunshan Ultrasonic Instruments Co., Ltd. (Jiangsu, China). An SC-3164 low speed centrifuge was from Anhui USTC Zonkia Scientific Instruments Co., Ltd., China. pH of sample solutions was determined with a pHS-3C digital pH meter (Shanghai Rex Instruments Factory, China).

The solid-state ^{1}H NMR and ^{13}C NMR spectra were obtained with an Infinityplus-400 spectrometer (Varian, USA). Mass spectra were obtained on a Bruker Esquire 3000 plus mass spectrometer (Bruker-Franzen Analytik GmbH Bremen, Germany) equipped with an ESI

interface and an ion trap analyzer. The static surface tension (γ) and contact angle (CA) were measured with an OCA20 apparatus (DataPhysics, Germany) at a saturated humidity with the temperature controlled by a superthermostat (Julabo F25, Germany).

DLS measurement was prepared by filtering solution through a 0.45 μm Millipore filter into a clean scintillation vial. The samples were examined on a laser light scattering spectrometer (BI-200SM) equipped with a Zetasizer Nano ZS instrument using a He-Ne laser at the wavelength of 632 nm (Malvern, UK) and a scattering angle of 90^{o}. The concentration of CDV was 0.05 mM and pH was in the range of 4.0–9.0. In addition, the hydrodynamic diameter (D_h) of CDV was determined in aqueous solutions by DLS.

SAXS spectra were determined using the SAXS beam line of the National Synchrotron Light Laboratory (LNLS, Campinas, Brazil). A position sensitive X-ray detector and a multichannel analyzer were used to determine the SAXS intensity. The X-ray scattering intensity, $I(q)$, was determined as a function of the scattering vector (q) which was given by $q = (4\pi/\lambda)\sin(\theta)$, where λ is the X-ray wavelength and θ is half the scattering angle.[1]

SEM images were acquired on an S4800 ESEM microscope (Hitachi, Japan). TEM images were recorded on an H600 electron microscope (Hitachi, Japan) with an accelerating voltage of 100 kV. The samples were diluted with ethanol and the specimens were dried at room temperature before determinations.

FT-IR spectra were obtained by a 670 FT-IR spectrometer (Thermo Nicolet, USA) in the range of 400–4000 cm^{-1} and the samples were measured until the final pressure was 0.004 mbar. Ultraviolet-visible (UV-Vis) absorption spectra were recorded using a Perkin Elmer UV-Vis spectrophotometer (USA) with a 1 cm path length quartz cuvette.

Thermogravimetric (TG) curves were carried out on a Q500 thermal gravimetric analyzer (TA Instruments Inc., USA) at the heating rate of 10 °C min^{-1} from room

temperature to 800 °C under flowing air. An X-ray photoelectron spectrometer (XPS, ESCALAB250, Thermo Electron Corporation, USA) was used to obtain XPS data.

The pore size distribution and specific surface area of the monoliths were obtained by N_2 adsorption-desorption experiments with an ASAP2020 accelerated surface area and porosimetry analyzer (Micromeritics, USA). The mesopore size distribution was evaluated from the desorption branches of isotherms based on the BJH (Barrett-Joyner-Halenda) model. Specific surface area values were determined by the BET (Brunauer-Emmett-Teller) equation at P/P_0 values between 0.01 and 0.98.

MALDI-TOF MS (Applied Biosystems, Foster City, CA) with a polished target was utilized for protein identifications. 7 mg mL^{-1} CHCA dissolved in a 2:1 (*v*/*v*) mixture of ACN/H_2O containing 0.1% (*v*/*v*) TFA was used as the matrix. MALDI-MS experiments were performed with constant laser intensity in the positive ion mode. All mass spectra were obtained with an accumulation of 1200 laser shot in the reflector mode with an accelerating voltage of 21.85 kV.

For UPLC-Orbitrap Tribrid Fusion MS analysis (Orbitrap Fusion Tribrid mass spectrometer, Thermo Fisher Scientific Company, USA), the spray voltage of MS was set at 2.0 kV, and the temperature of ion transfer capillary was 250 °C unless otherwise stated. The MS/MS spectra were acquired in the data-dependent mode, and the 20 most intense ions from the full scan were selected to fragmentation *via* higher-energy collisional dissociation (HCD) in the Orbitrap MS/MS. The experiments parameters were set as follows: spray voltage, 4000 V; sweep gas flow rate, 1.0 respective arbitrary units; sheath gas flow rate, 40 respective arbitrary units; aux gas flow rate, 10 respective arbitrary units; ion transfer tube temperature, 350 °C; vaporizer temperature, 200 °C; MS_1 detector, Orbitrap; MS_1 resolution, 120000; MS_1 scan range, 800–3500; MS_1 maximum injection time, 100 ms; MS_2 HCD collision energy, 45%; MS_2 detector, Orbitrap; MS_2 resolution, 15000; MS_2 maximum injection time, 35 ms;

and MS_2 start mass, 100. Xcalibur Qual and Quan browser software (Thermo Scientific, USA) were used for qualitative and quantitative analysis. All MS/MS spectra raw files by UHPLC-Orbitrap Fusion TMS analysis were converted to *.mgf file by Proteome Discoverer (version 1.4) and searched against International ProteinIndex (IPI) Human 3.8 database using MASCOT (version 2.3). The search criteria were set as follows: variable modifications of methionine oxidation (+15.995 Da), N-terminal acetylation, deamidation (N). fixed modification of cysteine residues (+57.022 Da), and at most two missed tryptic cleavage sites, MS tolerances were set as 20 ppm for parent ions and 0.5 Da for fragment ions. The false positive rates (FDRs) were controlled to be less than 1% for the identification of peptides, proteins, and glycosylation sites.

2. Construction of poly(GMA-PETA-CDV)

Prior to the preparation of monolithic columns, the inner wall of fused-silica capillaries (530 μm i. d. × 40 cm) were vinylized to enable the covalent attachmentas described in our previous study.[2,3] The inner wall was rinsed with 1 M NaOH for 30 min, water for 10 min, 1 M HCl for 30 min, water for another 10 min, and acetone for 10 min, successively. Then a solution of *γ*-MAPS/acetone (50%, *v*/*v*) was employed to modify the inner wall at 55 °C for 14 h. Afterward, the polymerization solution consisting GMA (480 mg), PETA (320 mg), PEG 20000 (160 mg), PEG 6000 (980 mg), H_2O (60 mg), AIBN (1% with respect to monomer, *w*/*w*), DMPA (1% with respect to monomer, *w*/*w*), and SH-CDV with different amounts was purged with N_2 for 10 min, ultrasonicated for 15 min to remove the dissolved O_2, and then inlet into the as-pretreated capillary. For the polymerization, the freshly synthesized SH-CDV was dispersed in the polymerization mixture and copolymerized with the monomer (GMA) *via* a thiol-epoxy click polymerization reaction by using DMPA and AIBN as the initiator.

Subsequently, the capillary was sealed by silicon rubbers at both ends and heated to 60 °C under UV radiation conditions for 24 h. Finally, the obtained monolith was washed with MeOH to remove the unreacted component and porogenic solvent overnight before use.

3. Sample preparation

Human blood samples from volunteers were obtained from China-Japan Hospital of Jilin University (Changchun, China). The collected serum samples were stored in separate glass tubes containing EDTA as an anticoagulant additive and then centrifuged (within 2 h of collection) at 4000 rpm for 10 min at 5 °C. The blood samples were subsequently stored at −20 °C and filtered by 0.22 μm film before use.

A blank blood sample (1 mL) was prepared by removing any potential Myo glycopeptides using the PMME process. The as-obtained residual blood sample was used as the blank serum sample. A series of samples were spiked with Myo in the concentration range of 0–5 pmol. For recovery tests, the samples were spiked with Myo with concentrations of 0.01 and 0.1 pmol, respectively. All samples were degassed and homogenized with an ultrasonic bath prior to analysis. For real sample analysis, human serum treated with trypsin digest was introduced into the PMME procedure.[4]

4. Myo digestion

1 mg Myo lyophilized powder was denatured by 1 mL PBS solution (50 mM, pH 7.4) and stored at −20 °C before use. Low concentration Myo solutions were prepared by diluting the stock solution with the above PBS solution to the final concentration and denatured at 100 °C for 15 min. Trypsin was added to the Myo solution at an enzyme/substrate mass ratio

of 1:30 and incubated at 37 °C overnight. Finally, FA (98%, *v*/*v*) was added to adjust pH to 2.0–3.0 and the reaction was terminated.

5. Calculation

(1) Myo-Loaded SH-CDV: Myo-loaded SH-CDVs were prepared as follows. A certain amount of Myo was added to a solution at pH 7.4, and then water was added until the volume of the solution reached 25 mL. The ultimate concentration of Myo was 0.01 μg mL^{-1}. Subsequently, the prepared Myo-loaded SH-CDV was purified by ultracentrifugation (10000 rpm for 2 min) and dialyzed (molecular weight cut off of 3500) in water for several times until the water outside the dialysis tube exhibited negligible Myo absorbance. The Myo encapsulation and loading capacities were calculated by the following equations:[5]

$$\textit{Encapsulation efficiency}\ (\%) = M_{\text{Myo-loaded}} / M_{\text{Myo}} \quad (1)$$

$$\textit{Loading capacity}\ (\%) = M_{\text{Myo-loaded}} / M_{\text{CDVs}} \quad (2)$$

where $M_{\text{Myo-loaded}}$, M_{Myo}, and M_{CDVs} are masses of Myo encapsulated in vesicles, added Myo, and Myo-loaded SH-CDV (mg), respectively. The mass of Myo was measured by a UV spectrophotometer at 214 nm and calculated relative to a standard calibration curve in water.

(2) Controllable Myo release: The release efficiency was monitored by the observed absorbance at 214 nm from the time-dependent UV-Vis spectroscopy. Trace amounts of HCl were added to decrease the pH values. The Myo release rate was calculated by the following equation:[6]

$$\textit{Release rate}\ (\%) = 1 - (C_0 - C_T) / (C_0 - C_M) \quad (3)$$

where C_M is the concentration of Myo in solution after adding SH-CDV and measured at pH 7.4, C_T is the concentration of Myo measured at pH 5.0, and C_0 is the initial concentration of Myo in solution (mg mL^{-1}). The pH treatment time for determination is 1 min for every pH

point.

(3) Permeability: The permeability of monoliths was described by the back pressure drop of the monolithic column and determined on a Waters 2489 liquid chromatography system equipped with Waters 1525 binary pumps (Waters, USA) at different flow rates using 70% ACN + 0.1% FA as the mobile phase. The permeability was calculated according to Darcy's Law:[7]

$$B_0 = \frac{F\eta L}{\pi r^2 \Delta p} \tag{4}$$

where F is the linear velocity of the eluent, η is the dynamic viscosity of the mobile phase (0.580 cP), L is the effective length of the column (μm), r is the inner radius of the column (μm), ΔP is the pressure drop across the column (bar), and B_0 is permeability (m^2). The value of B_0 can be used as an index for evaluating the permeability quality of monoliths.

(4) Swelling behavior: The poly(GMA-PETA-CDV) monolithic column was tested upon their swelling behavior in DMSO, known as an excellent solvent for organic polymers. The swelling propensity (*SP*) factor which was introduced by Nevejans and Verzele.[8]

$$SP = [p_{(DMSO)} - p_{(H2O)}] / p_{(H2O)} \tag{5}$$

where p is defined as the ratio of back pressure to solvent viscosity ($p = P/\eta$). $SP = 0$ implies that the material has a property of non-swelling and the higher is *SP* factor, the more the material swells.

(5) Dynamic binding capacity (*DBC*): *DBC* during the open-loop experiments was determined by the breakthrough area integration method and by the measurement of the quantity of the eluted component.[33] To determine *DBC* of poly(GMA-PETA-CDV) monolith for glycopeptides, frontal analysis of the monolith was carried out with 0.1 mg mL^{-1} Myo and 0.1 mg mL^{-1} BSA dissolved in PBS with pH at 5.0 and 7.4, respectively. *DBC* was calculated by the following equation:[9]

$$DBC = (V_B - V_0) \times C / m \quad (6)$$

where V_B is 10% breakthrough volume (mL), V_0 is the dead volume (mL), C is the protein concentration (mg mL^{-1}), and m is the weight of monolithic rod (mg). In brief, the monolith was equilibrated with loading buffer at pH 5.0. A sample solution containing 0.1 mg mL^{-1} Myo or BSA in PBS was pumped through the column at a flow rate of 50 μL min^{-1}. The dynamic breakthrough curve was recorded in a flow cell located in a UV spectrometer at 214 nm until 100% breakthrough was reached.

(6) Hemocompatibility assessment: Hemolysis ratio was measured to investigate the blood compatibility properties of poly(GMA-PETA-CDV) monolith. The value of hemolysis ratio was calculated according to the equation:

$$R_H = (A_t - A_{nc}) / (A_{pc} - A_{nc}) \quad (7)$$

where A_t is the absorbance of the sample at 214 nm, A_{pc} and A_{nc} are the absorbance of the positive and negative controls of purified water and normal saline (9%, *m*/*m*), respectively. R_H of poly(GMA-PETA-CDV) monolith was determined to be 0.45%, which was lower than the clinic limit, 5%. Such results implied that the materials conformed to the requirement of biomaterials.

(7) Matrix effect: Matrix effect (*ME*) of the PMME-MS method was investigated since it may have significant interference on the analysis process and affect the accuracy of analytical results. *ME* during validation of analytical methods in biological fluids can be examined as the following equation:

$$ME = (A_{MS} - A_M) / A_S \quad (8)$$

where A_S is the mass peak area of the standard solution (1 pmol Myo tryptic digests) in 70% ACN + 0.1% FA. A_M and A_{MS} are the mass peak areas of blank human blood sample and 1 pmol Myo tryptic digests in blank human blood sample obtained after the PMME procedure, respectively. If the *ME* value is above 1.0, there is signal enhancement, but if it is below 1.0,

there is signal suppression. If *ME* equals to 1.0, there is no matrix effect. In this study, *ME* values were determined (in triplicate) to be in the range of (0.87–1.18) ± 0.02, indicating that the matrix effects of human blood samples were low and could be ignored.[10]

6. SH-CDV formation and characterization

When **1** was dissolved in water, γ was measured as a function of the concentration of **1** (C) to determine its critical micelle concentration (CMC) in water (**Figure S2a**). There were two linear segments in the curve of γ *versus* C and a sudden reduction in the slope could be observed, implying that CMC is ~1.0×10^{-4} M.[6]

Figure S2b showed the autocorrelation functions and the average relaxation time (τ) calculated from the autocorrelation functions investigated with DLS measurements at pH 7.4 and 5.0, respectively. At pH 7.4, τ was ca. 0.23 ms, which was close to the value for CDVs and corresponded to a spherical object with a diameter of ~90 nm (**Figure S2c**). On the other hand, τ was ca. 0.33 ms at pH 5.0 corresponding to an object with a mean effective hydrodynamic diameter (D_h) of 100 nm, which could be a fiber in dimension of 8 nm × 400 nm. D_h could be calculated according to $D_h = L / \ln(L/d)$, where L and d are the length and diameter of the fiber (nm), respectively.

Figure S3a showed experimental SAXS intensities and fitting results of SH-CDV, indicating that the scattered peak signals were gradually weakened. The size of SH-CDV microsphere could be calculated by scattering peak of q value. Combined with the radical excess electron density of fitting result in **Figure S3b**, indicating SH-CDV has homogeneous in density with a narrow size distribution. The size was calculated to be approximately 110 nm, which was basically consistent with DLS measurements.

(1) Mansur, H. S.; Orefice, R. L.; Mansur, A. A. P. Characterization of Poly(vinyl alcohol)/poly(ethylene glycol) Hydrogels and PVA-derived Hybrids by Small-angle X-ray Scattering and FTIR Spectroscopy. *Polymer* **2004**, *45*, 7193–7202.

(2) Zheng, H. J.; Zhu, T. G.; Li, X. Q.; Ma, J. T.; Jia, Q. Peanut Agglutinin and β-Cyclodextrin Functionalized Polymer Monolith: Microextraction of IgG Galactosylation Coupled with Online MS Detection. *Anal. Chim. Acta* **2017**, *983*, 141–148.

(3) Zheng, H. J.; Ma, J. T.; Feng, W.; Jia, Q. Specific Enrichment of Glycoproteins with Polymer Monolith Functionalized with Glycocluster Grafted β-Cyclodextrin. *J. Chromatogr. A* **2017**, *1512*, 88–97.

(4) Zhang, H.; Lu, H. Y.; Huang, H. C.; Liu, J. C.; Fang, X. W.; Yuan, B. F.; Feng, Y. Q.; Chen, H. W. Quantification of 1-Hydroxypyrene in Undiluted Human Urine Samples Using Magnetic Solid-phase Extraction Coupled with Internal Extractive Electrospray Ionization Mass Spectrometry. *Anal. Chim. Acta* **2016**, *926*, 72–78.

(5) Wang, K.; Guo, D. S.; Wang, X.; Liu, Y. Multistimuli Responsive Supramolecular Vesicles Based on the Recognition of p-Sulfonatocalixarene and Its Controllable Release of Doxorubicin. *ACS Nano* **2011**, *5*, 2880–2894.

(6) Wang, J.; Chen, X.; Cui, W. L.; Yi, S. J. pH-Responsive Vesicles from Supra-Amphiphiles Based on Dynamic Imine Bond. *Colloids Surf., A* **2015**, *484*, 28–36.

(7) Zhao, Y. Y.; Yu, L.; Guo, Z. M.; Li, X. L.; Liang, X. M. Reversed-phase Depletion Coupled with Hydrophilic Affinity Enrichment for the Selective Isolation of N-Linked Glycopeptides by Using Click OEG-CD Matrix. *Anal. Bioanal. Chem.* **2011**, *399*, 3359–3365.

(8) Gosetti, F.; Mazzucco, E.; Zampieri, D.; Gennaro, M. C. Signal Suppression/enhancement in High-performance Liquid Chromatography Tandem Mass Spectrometry. *J. Chromatogr. A* **2010**, *1217*, 3929–3937.

(9) Boto, R. E. F.; Anyanwu, U.; Sousa, F.; Almeida, P.; Queiroz, J. A. Thiacarbocyanine as

Ligand in Dye-affinity Chromatography for Protein Purification. II. Dynamic Binding Capacity Using Lysozyme as a Model. *Biomed. Chromatogr.* **2009**, *23*, 987–993.

(10) Ma, J. F.; Liang, Z. Qiao, X. Q.; Deng, Q. L.; Tao, D. Y.; Zhang, L. H.; Zhang, Y. K. Organic-inorganic Hybrid Silica Monolith Based Immobilized Trypsin Reactor with High Enzymatic Activity. *Anal. Chem.* **2008**, *80*, 2949–2956.

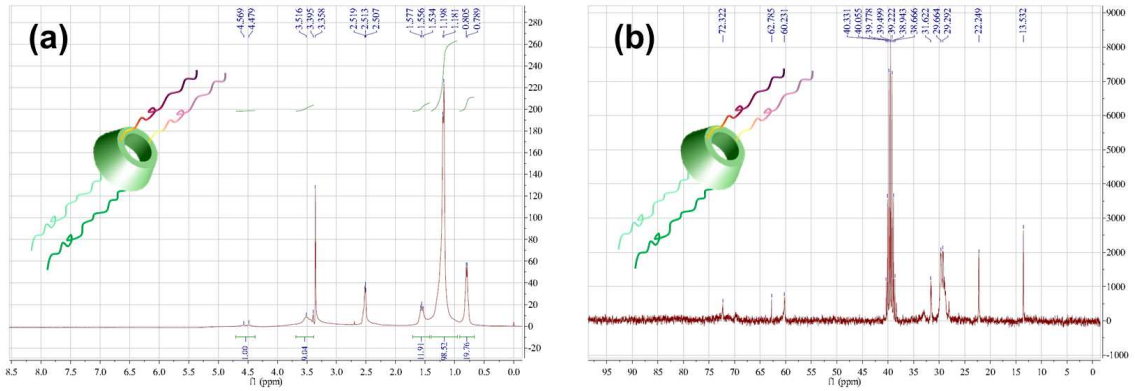

Figure S1. (a) ^{1}H NMR and (b) ^{13}C NMR of compound **1**.

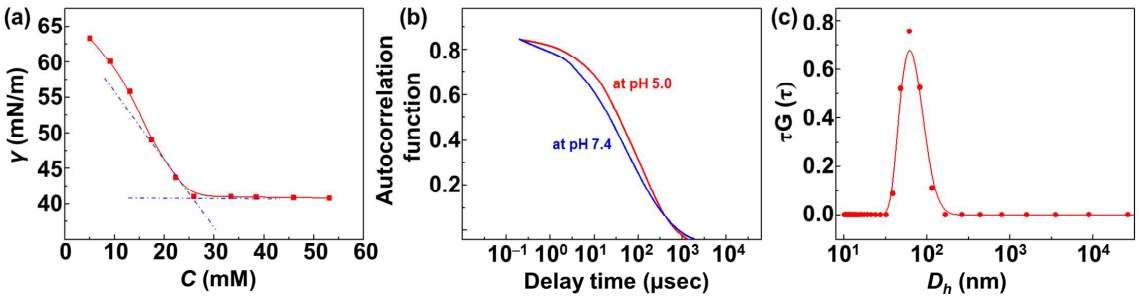

Figure S2. (a) Surface tension of **1**; (b) autocorrelation functions from DLS measurements performed on mixture of **1** (1 mM) and **2** (0.5 mM) at pH 7.4 and 5.0; and (c) D_h distribution determined by DLS for CDV at pH 7.4.

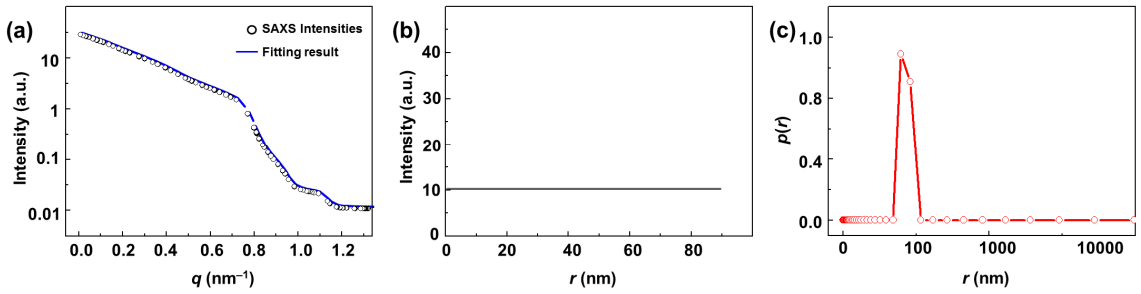

Figure S3. (a) Experimental SAXS intensities and fitting results of SH-CDV, (b) radical excess electron density of fitting result, and (c) *r* distribution determined by SAXS.

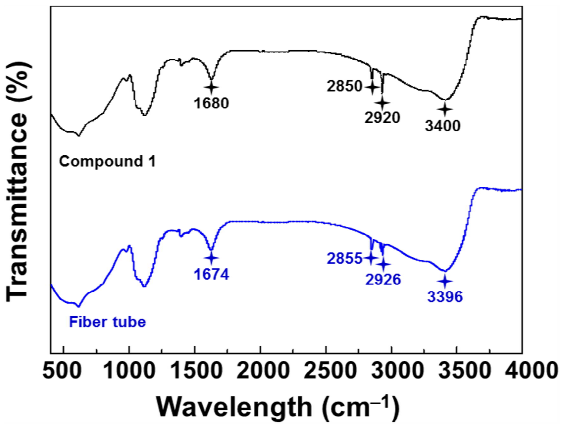

Figure S4. FT-IR spectra of compound **1** and fiber tube.

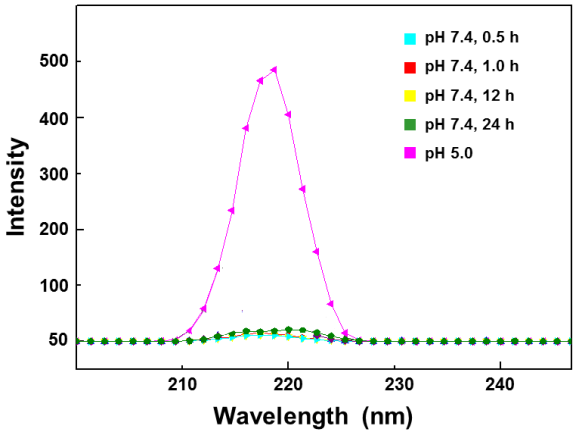

Figure S5. UV spectra of Myo encapsulated in a 1.0×10^{-4} M vesicular solution at pH 5.0 and at different aging times (0.5-24 h) when the pH was 7.4.

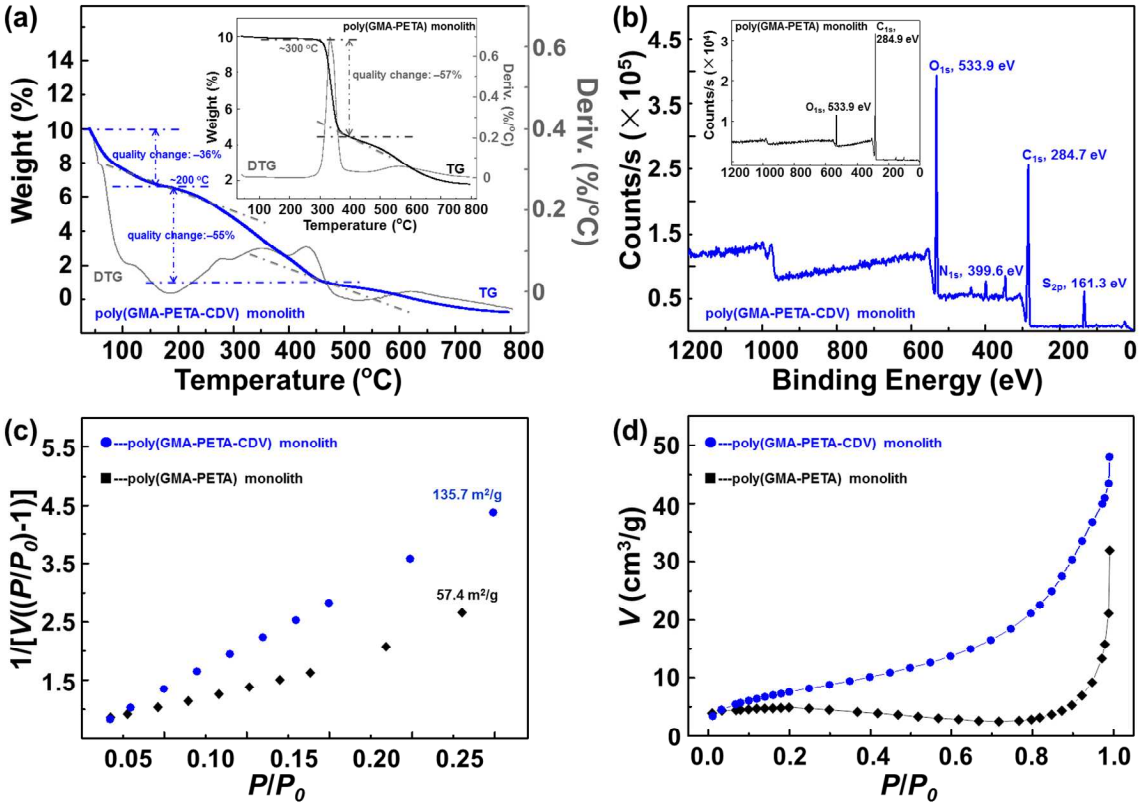

Figure S6. Characterization of poly(GMA-PETA) and poly(GMA-PETA-CDV) monoliths: (a) TG-DTG curves, (b) XPS spectra, (c) specific surface area, and (d) pore diameter distribution.

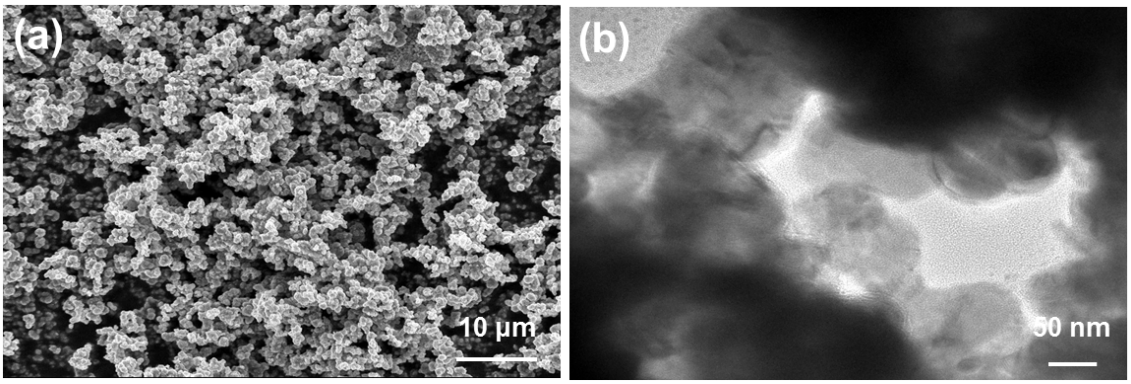

Figure S7. (a) SEM and (b) TEM images of poly(GMA-PETA-CDV) monolith after adjusting pH back to 7.4.

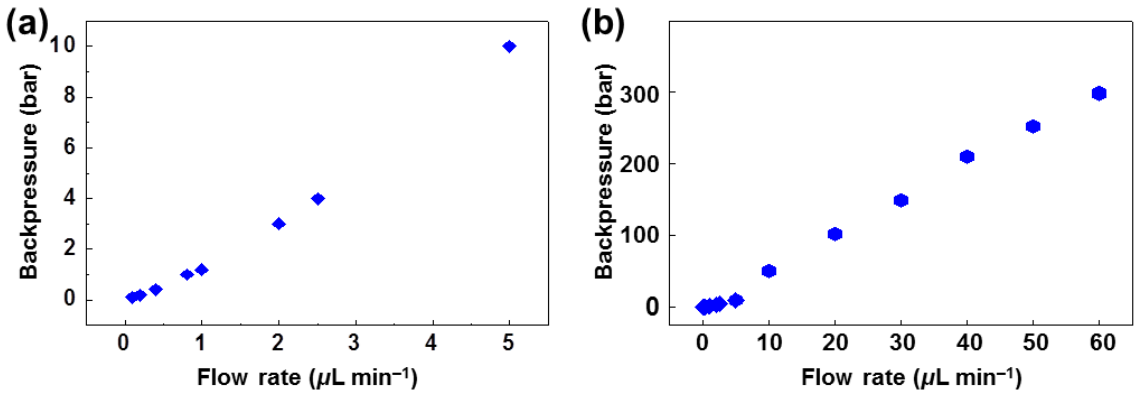

Figure S8. Relationship between flow rate and back pressure. Condition: 530 μm i. d., 3 cm length; room temperature; flow rate: (a) 0.1–5 μL min^{-1} and (b) 0.1–60 μL min^{-1}.

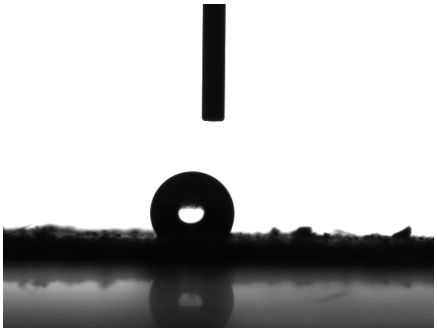

Figure S9. CA of poly(GMA-PETA-CDV) monolith (pH 5.0).

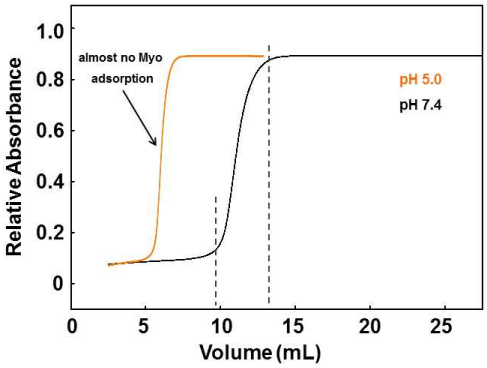

Figure S10. Breakthrough curves of Myo on poly(GMA-PETA-CDV) monolith.

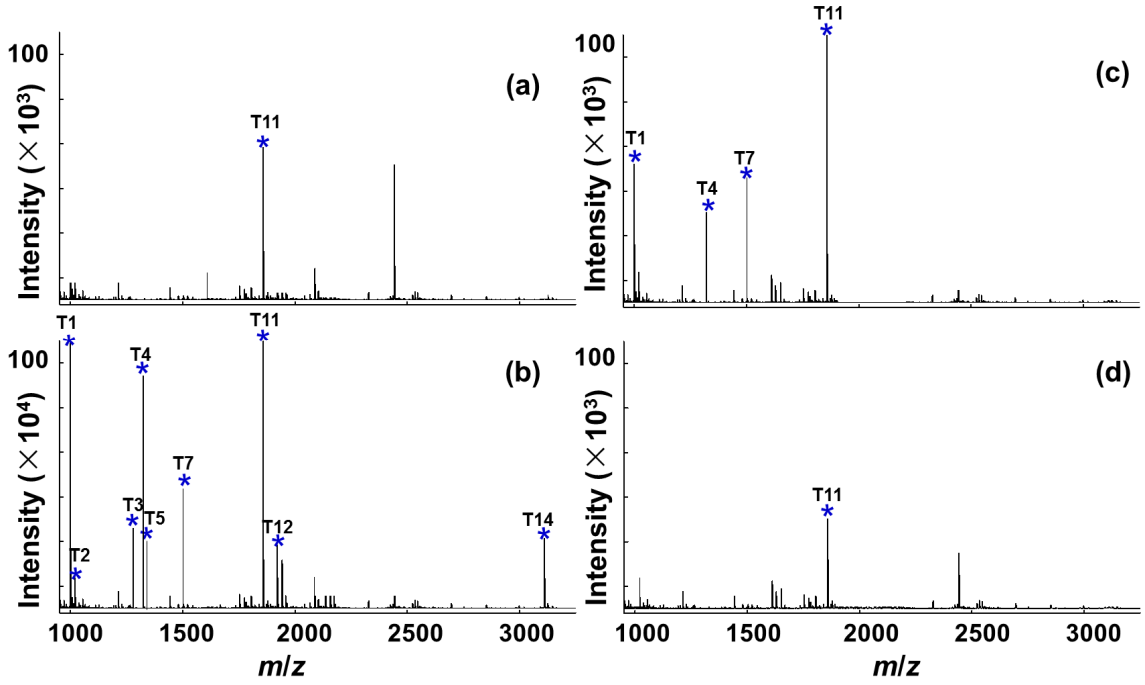

Figure S11. MALDI-MS spectra of Myo tryptic digests. (a) Enrichment by poly(GMA-PETA) monolith (10 fmol); and enrichment by poly(GMA-PETA-CDV) monolith: (b) 0.5 fmol, (c) 0.1 fmol, and (d) 0.05 fmol. Glycopeptides were marked.

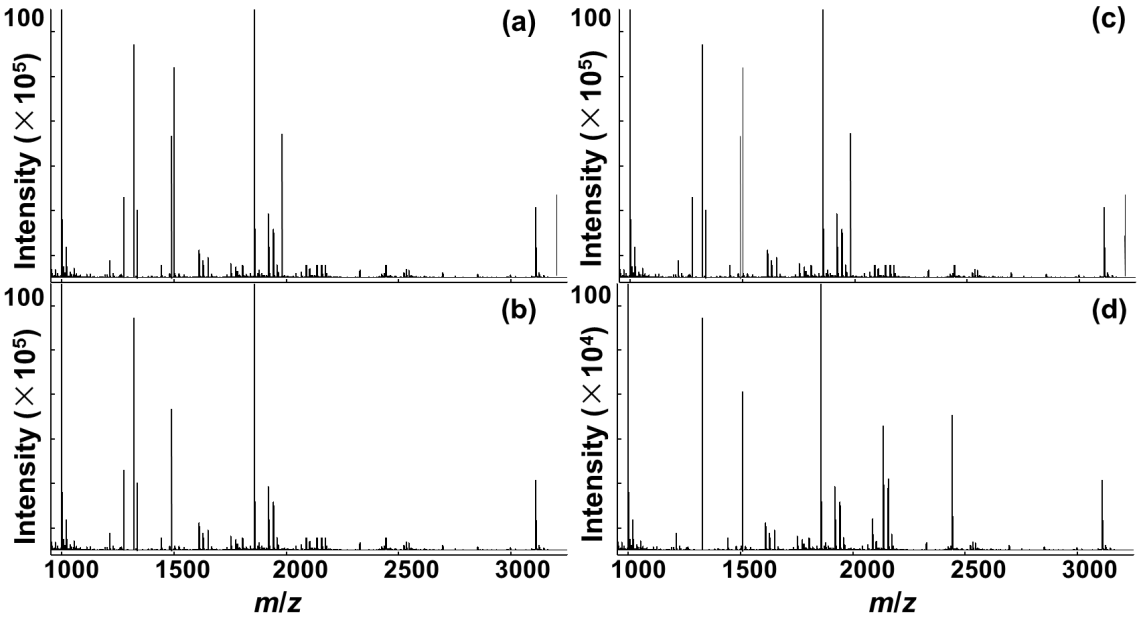

Figure S12. MALDI-MS spectra of Myo tryptic digests enriched by poly(GMA-PETA-CDV) monolith. (a) For the first time, (b) after 10 times, (c) after 50 times, and (d) after 90 times.

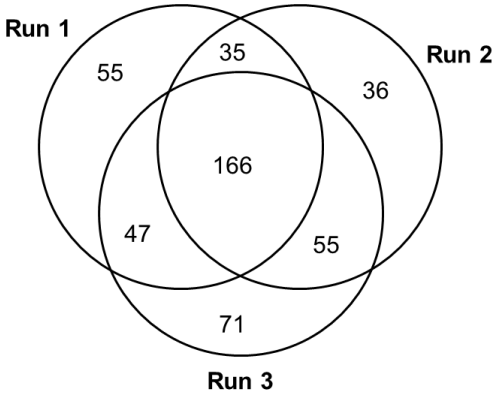

Figure S13. Overlap of the glycosylation sites identified by glycoproteome analysis of 1 μL human blood from UHPLC-Orbitrap Fusion TMS analyses.

Table S1 Recipes of monoliths (Polymerization time of 24 h and polymerization temperature of 60 ℃ under UV radiation conditions in all cases).

Column	(Monomer + Crosslinker) / Porogen	Monomer /Crossliner	PEG 20000 (*wt* %)	PEG 6000 (*wt* %)	H_2O	*SP*	Permeability ($\times 10^{-14}$ m^2)
1	5 / 5	6 / 4	35	60	5	0.54	0
2	2 / 3	6 / 4	25	70	5	0.50	1.14
3	2 / 3	6 / 4	15	80	5	0.49	3.34
4	2 / 3	9 / 1	25	70	5	0.47	6.27
5	2 / 3	9 / 1	20	75	5	0.36	7.98
6	2 / 3	9 / 1	13	82	5	0.32	10.89

Table S2 Molecular masses and amino acid sequence of Myo glycopeptides after enrichment.

Peak	*m*/*z*	Amino acid sequence
T1	942.05	K.YKELGFQG.–
T2	1087.28	K.HLKTEAEMK.A
T3	1272.43	R.LFTGHPETLEK.F
T4	1361.57	K.ALELFRNDIAAK.Y
T5	1379.67	K.HGTVVLTALGGILK.K
T6	1503.62	K.HPGDFGADAQGAMTK.A
T7	1507.85	K.HGTVVLTALGGILKK.K
T8	1607.79	K.VEADIAGHGQEVLIR.L
T9	1662.87	R.LFTGHPETLEKFDK.F
T10	1817.00	–.GLSDGEWQQVLNVWGK.V
T11	1887.13	K.YNEFISDAIIHVLHSK.H
T12	1938.22	R.LFTGHPETLEKFDKFK.H
T13	1983.22	K.KGHHEAELKPLAQSHATK.H
T14	3371.73	K.YNEFISDAIIHVLHSKHPGDFGADAQGAMTK.A
T15	3405.77	–.GLSDGEWQQVLNVWGKVEADIAGHGQEVLIR.L

Table S3 Comparison of different sample preconcentration and detection methods for the determination of Myo tryptic digests.

Method	Material	Detection method	LOD	Sample	Ref.
SPME	organic-inorganic hybrid monolith	μHPLC-ESI-MS/MS	10 fmol	E. coli	[33]
Immunosensor	AuNP/Br-Py/GCE	immunoassay	6.29 ng/mL	Blood serum	[27]
SPE	magnetic microspheres	cIEF[a]-ESI-MS/MS	70 fmol	Human serum	[34]
SPME	poly(EHMA-EDMA) monolith	LC-MALDI-MS	10 fmol	-	[35]
SPE	proPac SAX-10 column	HPLC-ESI-MS	460 fg/mL	Human serum	[36]
PMME	MAA-silica hybrid monolith	nano-RPLC-ESI/MS/MS	-	E. coli	[37]
PMME	poly(GMA-PETA-CDV) monolith	Orbitrap-MS	0.05 fmol	Human blood	This work

cIEF: capillary isoelectric focusing

Table S4 Comparison of different CD-based materials for glycoprotein analysis.

Material	Detection method	Glycoprotein	LOD	Sample	Ref.
CD-MOFs	MALDI MS	IgG	67 fmol	Mouse liver	[38]
β-CD-conjugated PDMS	fluoroimmunoassay	Myo	1.0 ng/mL	-	[26]
poly(MMA-HEMA-biotin-Lys-CD) monolith	MADLI MS	Plg	1.0 fmol	Human serum	[39]
poly(HEMA-EDMA-PNA-CD) monolith	Orbitrap MS	IgG	0.5 fmol	Human serum	[20]
poly(HEMA-PETA-glycoCD) monolith	MADLI MS	HRP	0.5 pmol	Human serum	[21]
poly(GMA-PETA-CDV) monolith	Orbitrap MS	Myo	0.1 fmol	Human blood	This work

Table S5. List of identified glycoproteins from 1 μL human blood sample captured by poly(GMA-PETA-CDV) monolith.

No.	Protein	Description	Sequence
1	IPI00123704	Atp1b2 Sodium/potassium-transporting ATPase subunit beta-2	K.KFHVN*YTQPLVAVK.F
			R.VINFYAGAN*QSM#NVTCVGKR.D
			K.FLEPYN*DSIQAQK.N
			R.VINFYAGAN*QSM#N* C G .R
			K.FLN*VTPNVEVNVECR.I
			K.TENLDVIVN*ISDTESWGQHVQK.L
			R.DEDAENLGHFVM#FPAN*GSIDLM#YFPYYGKK.F
2	IPI00122971	Ncam1 Isoform 1 of Neural cell adhesion molecule 1	R.TSTRN*ISSEEK.T
			R.DGQLLPSSN*YSNIK.I
3	IIPI00022431	AHSG cDNA	VCQDCPLLAPLNDTR
		FLJ55606, highly similar to Alpha-2-HS-glycoprotein	AALAAFNAQNNGSNFQLEEISR
4	IPI00129158	Sirpa Isoform 1 of Tyrosine-protein phosphatase non-receptor type substrate 1	R.VTN*VSDATKR.N
			K.VTQQSPTSM#NQVN*LTCR.A
			R.ISN*VTPEDAGTYYCVK.F
			K.NTDGTYN*YTSLFLVN*SSAHR.E
			K.NTDGTYN*YTSLFLVN*SSAHR.E
5	IPI00553177	SERPINA1 Isoform 1 of Alpha-1-antitrypsin	YLGNATAIFFLPDEGK
			ADTHDEILEGLNFNLTEIPEAQIHEGFQELLR
			QLAHQSNSTNIFFSPVSIATAFAMLSLGTK
6	IPI00123058	Cntn1 Contactin-1	R.GKAN*STGTLVITNPTR.I
			K.GTEWLVN*SSR.I
			R.YTCTAQTIVDN*SSASADLVVR.G
			R.GN*YSCFVSSPSITK.S
7	IPI00022429	ORM1 Alpha-1-acid	ENGTISR
		glycoprotein 1	NEEYNK
			QDQCIYNTTYLNVQR
8	IPI00118385	Grin1 Isoform 1 of Glutamate [NMDA] receptor subunit zeta-1	K.KVICTGPN*DTSPGSPR.H
			R.KLVQVGIYN*GTHVIPNDRK.I
			R.KDSPWKQN*VSLSILK.S
9	IPI00128360	Ntrk2 Isoform GP145-TRKB of BDNF/NT-3 growth factors receptor	K.HM#N*ETSHTQGSLR.I
			R.ITN*ISSDDSGK.Q

			R.LAAPN*LTVEEGK.S
			R.LEPNSVDPEN*ITEILIANQK.R
10	IPI00121550	Atp1b1 Sodium/potassium-transporting ATPase subunit beta-1	R.VLGFKPKPPKN*ESLETYPLMMK.Y
			K.YLQPLLAVQFTN*LTVDTEIR.V
			R.FKLDWLGN*CSGLNDDSYGYR.E
11	IPI00127556	Ncam2 Isoform Long of Neural cell adhesion molecule 2	K.SFN*ATAER.G
			R.KM#ILEIAPTSDNDFGRYN*CTATNR.I
			K.LLLPAKN*TTHLK.T
12	IPI00381178	Es31 Isoform 1 of Liver carboxylesterase 31	K.KNVN*ISYTVNDSFFPQRPQK.L
			K.NVN*ISYTVN*DSFFPQRPQK.L
13	IPI00321348	Igsf8 Immunoglobulin superfamily member 8	R.GETASLLCN*ISVR.G
			R.IGPGEPLELLCN*VSGALPPPGR.H
			R.LQAQDSGFYECYTPSTDTQYLGN*YSAK.V
14	IPI00378796	Adam22 Isoform 19 of Disintegrin and metalloproteinase domain-containing protein 22	R.TLN*CSGAHVK.L
			R.EICSGN*SSQCAPNVHK.M
			R.CLPVASFN*FSTCSSSK.A
15	IPI00022391	APCS Serum amyloid P-component	ESVTDHVNLITPLEKPLQNFTLCFR
16	IPI00130389	Dpp6 Dipeptidyl aminopeptidase-like protein 6	K.CEGPGVPTVTVHN*TTDK.R
			R.NVETNN*STVLIEGK.K
			R.AQN*VSILTLCDATTGVCTK.K
			R.NVETN*NSTVLIEGK.K
17	IPI00230013	Cacna2d1 Isoform 2B of Voltage-dependent calcium channel subunit alpha-2/delta-1	K.DAVNN*ITAK.G
			K.SFSGLLDCGN*CSR.I
			K.QSCITEQTQYFFKN*DTK.S
18	IPI00124830	Cd47 Isoform 2 of Leukocyte surface antigen CD47	R.DAM#VGN*YTCEVTELSR.E
			K.SYIFIYDGNKN*STTTDQN*FTSAK.I
			K.SYIFIYDGNKN*STTTDQN*FTSAK.I
19	IPI00128360	Ntrk2 Isoform GP145-TRKB of BDNF/NT-3 growth factors receptor	K.HM#N*ETSHTQGSLR.I
			R.ITN*ISSDDSGK.Q
			R.LAAPN*LTVEEGK.S
			R.LEPNSVDPEN*ITEILIANQK.R
20	IPI00108535	Ceacam1 Isoform Long of Carcinoembryonic antigen-related cell adhesion molecule 1	R.M#TLSQN*NSILR.I
			R.TLTLLN*VTR.N
			K.GN*TTAIDK.E

21	IPI00453537	Cadm2 Isoform 2 of Cell adhesion molecule 2	R.VDHESLN*ATPQVAM#QVLEIHYTPSVK.I R.ELNILFLN*KTDNGTYR.C R.ELNILFLN*KTDN*GTYR.C K.GSQGQFPLTQN*VTVVEGGTAILTCR.V
22	IPI00109727	Thy1 Thy-1 membrane glycoprotein	R.HEN*NTKDNSIQHEFSLTR.E K.VLTLAN*FTTK.D
23	IPI00018305	IGFBP3 Insulin-like growth factor-binding protein 3	AYLLPAPPAPGNASESEEDR GLCVNASAVSR
24	IPI00157497	Odz4 Isoform 3 of Teneurin-4	K.VGPYAN*TTR.Y R.LNGVN*VTYSPGGHIAGIQR.G R.LTN*VTFPTGQVSSFR.S
25	IPI00230289	Slc1a2 Isoform Glt-1A of Excitatory amino acid transporter 2	K.KVLVAPPSEEAN*TTK.A K.AVISM#LN*ETM#NEAPEETK.I
26	IPI00227126	Tnr Isoform 1 of Tenascin-R	K.GQCAN*GTCLCQEGYAGEDCSQRR.C R.GTN*ESEASSTQFTTEIDAPK.N
27	IPI00120245	Itgav Integrin alpha-V	K.AN*TTQPGIVEGGQVLK.C R.TAADATGLQPILNQFTPAN*VSR.Q R.IKTPEKN*DTGAAGQGER.S
28	IPI00115762	L1cam Neural cell adhesion molecule L1	K.VPGN*QTSTTLK.L K.VLLHHLDVKTN*GTGPVR.V R.THN*LTNLNPDLQYR.F K.EQLFFN*LSDPELR.T R.LLFPTN*SSSR.L
29	IPI00122974	Gpm6a Neuronal membrane glycoprotein M6-a	R.N*TTLVEGANLCLDLR.Q
30	IPI00121378	Alcam CD166 antigen	K.IIISPEEN*VTLTCTAENQLER.T R.LSLSEN*YTLSIANAK.I
31	IPI00122557	Gm4738 liver carboxylesterase 31-like isoform 1	K.NVN*ISYIVNDSFFPQRPEK.L K.NVN*ISYIVN*DSFFPQRPEK.L
32	IPI00409148	Hp Haptoglobin	K.NLFLN*HSETASAK.D K.VVLHPN*HSVVDIGLIK.L
33	IPI00316469	Stt3b Dolichyl-diphosphooligo saccharide--protein glycosyl transferase subunit STT3B	K.AM#SSN*ETAAYK.I R.TTLVDNNTWN*NSHIALVGK.A
34	IPI00113869	Bsg Isoform 2 of Basigin	K.TQLTCSLN*SSGVDIVGHR.W
35	IPI00230151	Mag Isoform S-MAG of Myelin-associated glycoprotein	R.ATAFN*LSVEFAPIILLESHCAAAR.D

			R.N*VTVN*ETEREFVYSER.S
			R.N*VTVN*ETEREFVYSER.S
36	IPI00111960	Gaa Lysosomal alpha-glucosidase	R.GVFITN*ETGQPLIGK.V
			R.LEN*LSSTESGYTATLTR.T
37	IPI00178926	IGJ Immunoglobulin J chain	ENISDPTSPLR
			IIVPLNNRENISDPTSPLR
38	IPI00114252	Ptgds Prostaglandin-H2 D-isomerase	K.TVVAPSTEGGLN*LTSTFLR.K
39	IPI00128454	Sez6l2 Isoform 2 of Seizure 6-like protein 2	R.IVSPEPGGAAGPN*LTCR.W
			R.LLAN*SSM#LGEGQVLR.S
40	IPI00157497	Odz4 Isoform 3 of Teneurin-4	K.VGPYAN*TTR.Y
			R.LNGVN*VTYSPGGHIAGIQR.G
			R.LTN*VTFPTGQVSSFR.S
41	IPI00131062	Scn1b Sodium channel subunit beta-1	K.DLQDLSIFITN*VTYN*HSGDYECHVYR.L
			K.DLQDLSIFITN*VTYN*HSGDYECHVYR.L
			R.VVWN*GSR.G
			R.LLFFDNYEHN*TSVVK.K
42	IPI00114939	Nptxr Neuronal pentraxin receptor	R.ALPGGTDN*ASAASAAGGSGPQR.S
43	IPI00119952	Gpm6b Isoform 1 of Neuronal membrane glycoprotein M6-b	K.SPQSN*GTSGVEQICVDVR.Q
44	IPI00881077	Lsamp Protein	K.LGVTN*ASLVLFKR.V
45	IPI00329927	Nfasc Neurofascin	K.QM#VENFSPN*QTK.F
			K.HNFRPGTDFVVEYIDSN*HTK.K
46	IPI00111013	Ctsd Cathepsin D	K.YYHGELSYLN*VTRK.A
47	IPI00222833	Lsamp Limbic system -associated membrane protein	R.GTDN*ITVR.Q
48	IPI00108844	M6pr Cation-dependent mannose-6-phosphate receptor	R.EASN*HSSGAGLVQINK.S
49	IPI00121190	Egfr Epidermal growth factor receptor	R.DCVSCQN*VSR.G
			K.DTLSIN*ATNIK.H
50	IPI00113824	Hspg2 Basement membrane-specific heparan sulfate proteoglycan core protein	R.ALVN*FTR.S
			R.SLTQGSLIVGNLAPVN*GTSQGK.F
51	IPI00469218	Lamp1 Putative uncharacterized protein	R.AFNISPN*DTSSGSCGINLVTLK.V
			R.GYLLTLN*FTK.N
52	IPI00118380	Grin2a Glutamate [NMDA] receptor subunit epsilon-1	K.INN*STNEGM#NVK.K
			R.FGTVPN*GSTER.N
53	IPI00109612	Lamb2 laminin subunit beta-2 precursor	R.AQAALDKAN*ASR.G
54	IPI00115599	Hsd11b1 Corticosteroid 11-beta -dehydrogenase isozyme 1	K.QSN*GSIAVISSLAGK.M

55	IPI00157497	Odz4 Isoform 3 of Teneurin-4	K.VGPYAN*TTR.Y
			R.LNGVN*VTYSPGGHIAGIQR.G
			R.LTN*VTFPTGQVSSFR.S
56	IPI00623371	Bcan Brevican core protein	K.TLFLFPN*QTGFPSK.Q
57	IPI00400016	Lamc1 Laminin subunit gamma-1	R.VNDN*KTAAEEALR.R
			R.IASAVQKN*ATSTK.A
58	IPI00119809	Lgals3bp Galectin-3-binding protein	K.APIPTALDTN*SSK.T
			R.ALGYEN*ATQALGR.A
59	IPI00022731	APOC4 Apolipoprotein C-IV	ELLETVVNR
60	IPI00420955	Sort1 Isoform 1 of Sortilin	K.DITNLIN*NTFIR.T
			R.HLYTTTGGETDFTN*VTSLR.G
61	IPI00108041	Stim1 Stromal interaction molecule 1	R.LAVTN*TTM#TGTVLK.M
62	IPI00119299	Lifr Isoform 1 of Leukemia inhibitory factor receptor	R.IEGLTN*ETYR.L
			R.KVPSN*STETVIESDQFQPGVR.Y
63	IPI00624663	Pzp Uncharacterized protein	K.VN*LSFPSAQSLPASDTHLK.V
			K.SLGEVN*FTATAEALQSPELCGNK.L
64	IPI00116921	Scarb1 Scavenger receptor class B member 1	R.ESGIQN*VSTCR.F
			K.LTYN*ESR.V
65	IPI00124221	Atp1b3 Sodium/potassium-transporting ATPase subunit beta-3	K.LVEDLESFLKPYSVEEQKN*LTSCPDGAPFIQHGPDYR.A
66	IPI00109153	Slc17a7 Vesicular glutamate transporter 1	R.CNLGVAIVSM#VN*NSTTHR.G
			R.CNLGVAIVSM#VNN*STTHR.G
67	IPI00022429	ORM1 Alpha-1-acid glycoprotein 1	ENGTISR
			NEEYNK
			QDQCIYNTTYLNVQR
68	IPI00321190	Psap Sulfated glycoprotein 1	K.TN*SSFIQGFVDHVK.E
			K.TVVTEAGNLLKDN*ATQEEILHYLEK.T
69	IPI00117803	Astn1 Isoform 2 of Astrotactin-1	R.ASPIYELVTNN*QTQR.L
70	IPI00128826	Cacng8 Voltage-dependent calcium channel gamma-8 subunit	R.ALICN*TTN*LTAGDDGPPHR.G
			R.ALICN*TTN*LTAGDDGPPHR.G
71	IPI00930854	Nfasc neurofascin isoform 3 precursor	K.QMVENFSPN*QTK.F
			K.VLTNNPYN*DSSLR.N
72	IPI00229992	Plxnb1 Plexin-B1	K.YTSDPN*VTSVGPSK.S
			R.VVAVSPAN*ISR.E
73	IPI00136967	Gria2 Isoform 1 of Glutamate receptor 2	K.RIN*YTINIM#ELK.T

74	IPI00785414	H2-K1 MHC class Ia H2-K antigen (Fragment)	K.NGN*ATLLR.T R.TLLGYYN*QSK.G
75	IPI00153840	Cadm4 Cell adhesion molecule 4	R.QTLFFN*GTR.A
76	IPI00022418	FN1 Isoform 1 of Fibronectin	LDAPTNLQFVNETDSTVLVR DQCIVDDITYNVNDTFHK LDAPTNLQFVNETDSTVLV
77	IPI00121362	F11r junctional adhesion molecule A precursor	R.AFM#N*SSFTIDPK.S
78	IPI00139788	Trf Serotransferrin	K.N*STLCDLCIGPLK.C
79	IPI00222429	Nomo1 Nodal modulator 1	R.VTNSNANAAGPLIVAGYN*VSGSVR.S
80	IPI00113528	Tm9sf3 Transmembrane 9 superfamily member 3	R.IVDVN*LTSEGK.V
81	IPI00116355	Gfra2 GDNF family receptor alpha-2	R.NAIQAFGN*GTDVNM#SPK.G
82	IPI00134691	Ugt1a1;Ugt1a2 UDP-glucuronosyltransferase 1-1	K.EN*VTATLVELGR.T
83	IPI00418163	C4B;C4A complement component 4B preproprotein	FSDGLESNSSTQFEVK
84	IPI00132600	Npc1 Niemann-Pick C1 protein	R.LIASN*ITETM#R.S
85	IPI00138061	Cr1l Isoform 1 of Complement regulatory protein Crry	R.IN*YTCNQGYR.L
86	IPI00117630	Itpr1 Isoform 7 of Inositol 1,4,5-trisphosphate receptor type 1	R.VETGEN*CTSPAPK.E
87	IPI00136642	Serpinc1 Antithrombin-III	K.LGACN*DTLK.Q
88	IPI00123920	Serpina1c Alpha-1-antitrypsin 1-3	K.GDTHTQILEGLQFN*LTQTSEADIHK.S
89	IPI00121038	Vcan Isoform V0 of Versican core protein	R.FEN*QTCFPLPDSR.F
90	IPI00110598	Gabra2 Gamma-aminobutyric acid receptor subunit alpha-2	K.SVAHN*MTM#PNK.L
91	IPI00222921	Slc9a7 Isoform 1 of Sodium/hydrogen exchanger 7	R.AFSTLLVN*VSGK.F
92	IPI00296608	C7 Complement component C7	NYTLTGR INNDFNYEFYNSTWSYVK
93	IPI00122257	Nt5e 5'-nucleotidase	R.IKLDN*YSTQELGR.T
94	IPI00154056	Acp2 Lysosomal acid phosphatase	R.YEQLQN*ETR.Q
95	IPI00123613	Pacsin1 Protein kinase C and casein kinase substrate in neurons protein 1	K.KAEGATLSN*ATGAVESTSQAGDR.G
96	IPI00409336	Gabbr2 Gamma-aminobutyric acid type B receptor subunit 2	R.IQDFN*YTDHTLGR.I
97	IPI00109108	Stt3a Putative uncharacterized protein	R.TILVDN*NTWN*NTHISR.V R.TILVDN*NTWN*NTHISR.V
98	IPI00228680	Nrxn3 neurexin III	R.INCN*SSKGPETLYAGQK.L
99	IPI00131091	C4a;C4b Complement C4-B	K.ALN*VTLSSM#GR.N
100	IPI00022463	TF Serotransferrin	CGLVPVLAENYNK QQQHLFGSNVTDCSGNFCLFR

101	IPI00119035	Acan Aggrecan core protein	R.TVYLHAN*QTGYPDPSSR.Y
102	IPI00120066	Prom1 Isoform 1 of Prominin-1	K.SLQDAATQLNTN*LSSVR.N
103	IPI00113726	Lama1 Laminin subunit alpha-1	R.VCDGN*STNPR.E
104	IPI00225153	Shisa7 Isoform 1 of Protein shisa-7	R.LTGALAGGGSAAGTSAN*ATK.T
105	IPI00170303	Lgi2 Isoform 1 of Leucine-rich repeat LGI family member 2	R.SYDN*ITGQSIVGCK.A
106	IPI00408895	Tgoln1 Trans-Golgi network integral membrane protein 1	R.RQPEKTDAELN*ETARPLSPVNPK.L
107	IPI00122048	Atp1a3 Sodium/potassium-transporting ATPase subunit alpha-3	K.GVGIISEGN*ETVEDIAAR.L
108	IPI00129159	Neo1 Isoform 1 of Neogenin	R.TPASDPHGDN*LTYSVFYTK.E
109	IPI00330887	Negr1 Neuronal growth regulator 1	R.SILTVTN*VTQEHFGN*YTCVAANK.L R.SILTVTN*VTQEHFGN*YTCVAANK.L
110	IPI00134191	Slc2a3 Solute carrier family 2, facilitated glucose transporter member 3	K.DFLN*YTLEER.L
111	IPI00876200	AI593442 Uncharacterized protein C11orf87 homolog	R.TFASHN*ASGGSSAGLR.S
112	IPI00309191	Unc5c Isoform 1 of Netrin receptor UNC5C	R.LSDTAN*YTCVAK.N
113	IPI00471081	Plbd1 Putative phospholipase B-like 1	R.DQGN*VTDM#ASM#K.Y
114	IPI00120302	Lgi1 Leucine-rich glioma-inactivated protein 1	K.ATQLFTN*QTDIPNMEDVYAVK.H
115	IPI00131995	Hapln1 Hyaluronan and proteoglycan link protein 1	R.GGN*VTLPCK.F
116	IPI00969516	LOC100293534 similar to complement component 4B (Childo blood group), partial	GLNVTLSSTGR
117	IPI00553387	Grm5 glutamate receptor, metabotropic 5 isoform a	K.TCN*SSLTLR.T
118	IPI00128358	Insr Insulin receptor	K.HN*LTITQGK.L
119	IPI00136925	Igj Immunoglobulin J chain	R.EN*ISDPTSPLR.R
120	IPI00120115	S1pr1 sphingosine 1-phosphate receptor 1	R.HYN*YTGK.L
121	IPI00396687	Dpp10 inactive dipeptidyl peptidase 10	R.WIN*DTVVVYK.T
122	IPI00224752	Atrn Attractin	R.GICN*ASDTR.G
123	IPI00356667	Pcdh17 protocadherin 17 precursor	K.DSGAPAHLESN*ATVR.V
124	IPI00331564	Dld Putative uncharacterized protein	K.TVCIEKN*ETLGGTCLNVGCIPSK.A
125	IPI00418153	IGHM Putative uncharacterized protein DKFZp686I15212	EEQYNSTFR
126	IPI00123342	Hyou1 Hypoxia up-regulated protein 1	R.VFGSQN*LTTVK.L
127	IPI00314726	Naglu alpha-N-acetylglucosaminidase	R.LLLTAAPN*LTTSPAFR.Y
128	IPI00342158	Nup210 Nuclear pore membrane glycoprotein 210	K.GATN*NTCIIR.T
129	IPI00291262	CLU Isoform 1 of Clusterin	MLNTSSLLEQLNEQFNWVSR ELPGVCNETMMALWEECKPCLK

130	IPI00896380	IGHM Isoform 2 of Ig mu chain C region	MLNTSSLLEQLNEQFNWVS KKEDALNETR HNSTGCLR EDALNETR KEDALNETR LANLTQGEDQYYLR NNSDISSTR YKNNSDISSTR THTNISESHPNATFSAVGEASICEDDWNSGER GLTFQQNASSMCVPDQDTAIR